arXiv:1704.05239v1 [cs.CV] 18 Apr 2017

Robust Optical Flow Estimation in Rainy Scenes

Li Ruoteng[1], Robby T. Tan[1,2], and Loong-Fah Cheong[1]

[1]National University of Singapore
[2]Yale-NUS

Abstract

This paper presents a method to estimate optical flow under rainy scenes. Optical flow estimation in the rainy scenes is considered challenging due to background degradation introduced by rain streaks and rain accumulation effects in the scene. Rain accumulation effect refers to poor visibility of remote object due to the intense rainfall. Most existing optical flow methods are erroneous when applied to rain sequences because the conventional brightness constancy constraint (BCC) and gradient constancy constraint (GCC) generally break down in this situation. In this paper, our method considers the rain streaks and rain accumulation separately. Based on the fact that the RGB color channels receive raindrop radiance equally, we introduce a residue channel as a new data constraint to significantly reduce rain streaks. In the case of rain accumulation, our method proposes to separate the image into a piecewise-smooth background layer and a high-frequency detail layer and enforce BCC on the background layer only. Results on both synthetic dataset and real images show that our algorithm outperforms existing methods on different types of rain sequences. To our knowledge, this is the first optical flow method dealing with rain.

1. Introduction

Optical flow methods have been developed for many decades, and achieved significant results in terms of accuracy and robustness. They are shown to generally work when applied to outdoor scenes in clear daylight. However, under realistic outdoor conditions, a range of dynamic weather phenomena such as rain, snow, and sleet will pose a grim problem for these methods. To our knowledge, no methods have been proposed to handle optical flow estimation under rainy scenes. We consider addressing this problem is important, since more and more vision systems, such as self-driving cars and surveillance, are deployed in outdoor scenes, and rain is an inevitable natural phenomena or even an everyday occurrence in some regions of the world. In this paper, we develop an algorithm that can handle rain in optical flow estimation. In the following, our discussion will be focused on rain, though the discussion and the resulting formulation are generally applicable to other dynamic weather condition such as snow and sleet. (Some examples and experiments on snow and sleet can be found in our supplementary material)

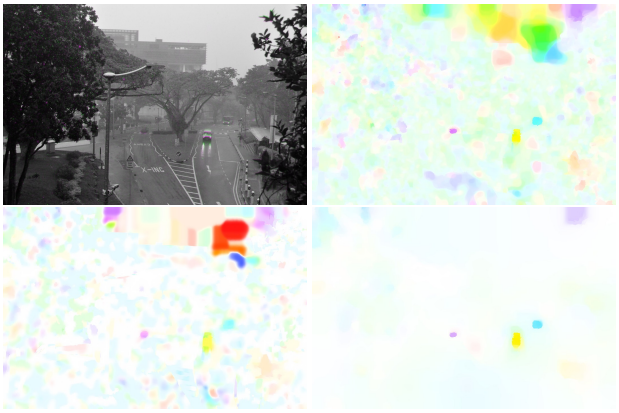

Figure 1: **Top Left:** Overlaid real rain image pair. This sequence background is static with some objects movement. The left black car moves upward and the right van moves downward. The remote bus moves left and the top right tree branch swings upward. **Top Right:** flow field of classic+NL [16]. **Bottom Left:** flow field of SPM-BP [12]. **Bottom Right:** flow field of our algorithm

The challenge of estimating optical flow in rainy scenes can be categorized into two problems. One problem refers to rain streaks, which due to their dynamic nature, appear in different locations from frame to frame, thus causing violation to the brightness constancy constraint (BCC). The spurious gradients created by the rain streaks also pose problem for the application of the gradient constancy constraint. The other problem refers to the rain streak accumulation (see

Fig. 1). Visually rain streaks throughout some space are accumulated and we can no longer see the streaks individually (visually this is similar to fog). Images affected by rain accumulation generally suffer from a veiling effect, and thus low contrast. Under torrential downpour or heavy snow, this second problem is severe enough to warrant a special mechanism to come to grips with the issue. Existing optical flow methods usually do not consider these degradation effects, and hence fail to produce satisfactory results.

Most existing optical flow methods rely on the brightness and gradient constancy constraints, which in rainy scenes do not hold anymore or become highly susceptible to noise due to the two aforementioned problems. Various robust statistics measures proposed by the community [3][2][18][16] help treat limited noise from rains, but do not work robustly on image degradation as strong and complex as heavy rains. A direct solution is to apply a deraining method before optical flow computation. However, most of the video-based deraining methods are designed only for rain streaks removal, and assume static background. Crucially for the optical flow estimation problem, most of these image-based deraining methods process each frame independently, and therefore consistency across frames cannot be guaranteed. Moreover, most of the deraining methods introduce artifacts, such as blur around the rain streak region, high frequency texture loss, image color change, etc. These artifacts are also inconsistent in their appearance throughout an image sequence, thus rendering the brightness constancy constraint invalid.

In this paper, our goal is to develop an optical flow algorithm that can work robustly and accurately in the presence of rain streaks and rain accumulation. To achieve this goal, our idea is based on the observation that the radiance of most raindrops has the same intensity on each RGB channel. Hence, by subtracting the maximum channel by the minimum channel of the rain image, we can reduce the rain streak influence in the resultant map (which we call the residue channel). Besides, to handle rain accumulation, we use image decomposition to separate the image into a piecewise-smooth background layer which captures the diagnostic structure of the image, and a high-frequency detail layer which contains the noise, rain, and the fine local details of the background.

Our contributions in this paper are (1) analysis on rain effects on optical flow, and how some state-of-the-art methods can cope with rain; (2) proposed residue channel for reducing the effect of rain streaks; (3) a layer separation scheme to extract the principal structure of the image, with the latter providing more reliable information under low contrast.

2. Related Work

Optical flow algorithms that are robust to noise and outlier have been studied for a long time [3][2][18][16]. While these techniques may be able to handle a moderate amount of corruptions such as those brought about by a drizzle, they are not likely to prevail against the heavy corruptions caused by a torrential downpour. Brox et al. [4] utilizes the gradient constancy constraint (GCC) to improve robustness against illumination change. However, in rainy scenes, rain streaks create spurious gradients which violate the gradient constancy constraint. Compounding these issues is the loss of contrast caused by rain accumulation; it renders both the brightness constancy constraint and gradient constancy constraint highly susceptible to noise.

One of the popular practices in optical flow estimation is to perform some kind of layer separation. Trobin et al.'s [17] is the first work to introduce structure-texture decomposition denoising [15] into the computation of optical flow. The purpose is to remove shadow and shading from the texture layer. However, for rainy scenes, high frequency rain streaks will appear in the texture layer and compromise the utility of the texture layer for flow estimation. A recent work by Yang et al.'s [1] proposed a double-layer decomposition framework to handle transparency or reflection, based on the assumption that both layers obey sparse image gradient distributions. This method cannot be used to remove the rain layer since the rain streaks result in a lot of gradients.

Mileva et.al's [14] proposed an illumination-robust variational method using color space transformation to handle shadow and highlights. Unfortunately, the HSV colour space and $r\phi\theta$ color space approaches do not result in measures that are invariant under the effects of rain streaks and hence cannot be directly applied to rainy scenes.

It is beyond the scope of this paper to offer a comprehensive review of the immense optical flow estimation literature, but the emerging deep learning approach certainly deserves a mention. Several Convolutional Neural Network(CNN) approaches [7][6][10] demonstrate the possibility of using a deep learning framework to estimate flow, but these methods are meant for optical flow estimation under normal scenes. CNN-based methods are heavily optimized over a lot of training data. Unfortunately, obtaining the optical flow ground-truths for rainy scenes is not easy. This issue is compounded if we want the method to be applicable to not just rain but a variety of dynamic weather phenomena such as snow and sleet. In contrast, our method leverages on the physics of the image formation process; theoretically, it can offer a much more parsimonious solution to a range of problems posed by different weather phenomena.

A number of single-image rain streaks removal algorithms have been proposed [11][13][20]. Kang et al. [11] decomposes an input image into low frequency (rain streak free) and high frequency components, and subsequently extracted geometric details from the high frequency component to recover the de-rained image. Yu et al.'s method [13],

Figure 2: Original image and its residue channel. **Left**: Image captured in a rainy scene with strong rain streaks. **Right**: Residue channel of this image.

decomposes the rain image into a rain-free background image layer and a rain streak layer and solves this formulation by introducing GMM prior of the background and rain streaks. The most recent single image rain streak removal work by Yang et al. [20] incorporates the convolutional neural network to learn the binary rain region feature and rain streak intensity feature. In the output image of traditional de-rain algorithms [11][13], the rain streak regions are blurred, and the background geometric details cannot be thoroughly recovered. The output image of CNN approach [20] has color change. Hence,the de-rained sequences of both approaches violate both BCC and GCC. Our experiments demonstrate that preceding the optical flow estimation with a state-of-the-art de-rain pre-processing step does not work well due to the artifacts introduced by the de-rain algorithms.

3. Residue Channel

Existing methods do not perform well on the sequences in rainy scenes because they are sensitive to the effect introduced by rain streaks. Our purpose of proposing residue channel is to reduce the effect of rain streaks based on the fact that the radiance of a raindrop has equal intensity in each RGB channel[21]. The appearance of rain streaks is caused by the movement of raindrops during the camera exposure[9]. If we assume the exposure time is T and the elapsed time while a raindrop is passing through a pixel is τ, the rain image I captured by the camera is a linear combination of the average raindrop radiance $\bar{E}_r$ and the background radiance E_b:

$$I(\mathbf{x}) = \tau \bar{E}_r(\mathbf{x}) + (T - \tau)E_b(\mathbf{x}), \tag{1}$$

where

$$\bar{E}_r = \frac{1}{\tau}\int_0^{\tau} E_r \mathbf{d}t, \quad 0 <= \tau <= T.$$

E_r is the radiance of the raindrop at a particular time. Following [21], the radiance of a raindrop on each chromatic channel is the same:

$$\bar{E}_r^R = \bar{E}_r^G = \bar{E}_r^B. \tag{2}$$

For a rain image I, we define

$$I_{res}(\mathbf{x}) = I^M(\mathbf{x}) - I^m(\mathbf{x}), \tag{3}$$

where I^M and I^m are the maximum-intensity color channel and minimum-intensity color channel of the rain image I respectively. We call I_{res} the *residue channel* of image I as shown in Fig. 2.

By combining Eq.(1) and Eq.(2), the radiance due to the raindrops is cancelled:

$$I_{res} = (T - \tau)(E_b^M - E_b^m).$$

Thus, the residue channel has a linear correlation with the channel difference of the background radiance.

$$I_{res} = \alpha(E_b^M - E_b^m), \tag{4}$$

where $\alpha = T - \tau$ and $0 <= \alpha <= T$.

We consider the residue channel to be more robust to rain than the RGB channel for optical flow estimation. In order to verify this, we captured rain images and clean images of the same scenes. We manually crop and register the flat blue sign board patch from all the collected images (Fig. 4). We calculate the variances of all the clean patches and the rain patches in both the RGB channel and the residue channel. Fig. 4 shows the sporadic noise points introduced by the rain streaks in residue channel is much smaller than that in the original rain image. Based on these observation we could see that the intensity variance of the residue channel is considerably smaller than that of the RGB channel. The rain streaks have been significantly reduced in the residue channel. This is a strong support to our residue channel hypothesis.

Rain images typically have severe rain accumulation effect particularly in the heavy rainy scenes (*e.g.* the remote objects in Fig. 3, Left). For each pixel, the intensity contributed by the rain is the accumulation of all the raindrops along the line of sight from the camera to the corresponding background object. We model the pixel intensity on rain image by taking the summation of the radiance of the background object and radiance due to all the rain drops passing through this pixel location during the exposure time.

$$I(\mathbf{x}) = \sum_i^N \alpha_i \bar{E}_i(\mathbf{x}) + (1 - \sum_i^N \alpha_i)E_b(\mathbf{x}), \tag{5}$$

where α_i denotes the contribution of the radiance of each raindrop to the entire radiance received by the camera. Because of light scattering and attenuation, the rain image will result in low contrast as shown in Fig. 5 Left. Taking the residue channel of this image, the contrast turns out to be even lower as shown in Fig. 5 Right. In the low contrast images with significant rain accumulation, the background texture cannot provide reliable matching due to the noise

Figure 3: Rain streaks and rain accumulation effect on images of rainy scenes. **Left**: Rain image with heavy rain accumulation effect. The visibility of the sign board is poor. **Right**: Rain image with rain streaks.

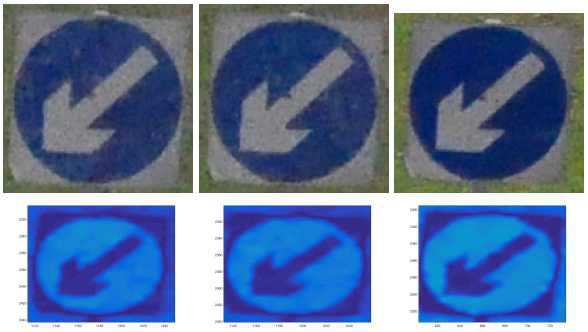

Figure 4: Rain streaks comparison in observed images and residue channels. Upper row shows the observed images. Lower row is their residue channels. **Left:** A sign board captured in rain at time t. **Middle:** The same sign board captured in rain at time t+1. The rain streaks are at different locations in these two images. **Right:** Sign board captured in clear daytime. One may find the rain streaks are significantly reduced in the circle area of the sign board.

and raindrops. We can only rely on information supplied by the coarse version of the principal regions of the image, including the object boundaries. For this purpose, we embed in our method a decomposition step that separates the image into a piecewise-smooth layer and a fine-details layer.

4. Proposed Method

4.1. Residue Map

In the variational framework, the optical flow objective function is expressed as:

$$E(I_1, I_2, \mathbf{u}) = \| I_1(\mathbf{x}) - I_2(\mathbf{x}+\mathbf{u}) \|^2 + \lambda_s(||\nabla \mathbf{u}||^2), \quad (6)$$

Figure 5: Sign board under heavy rain accumulation. **Left**: sign board captured in a rainy scene with heavy rain accumulation. **Right**: residue channel of this sign board image. For a better visibility, the residue channel has been scaled to [0,255]. The contrast of residue channel is poorer than the original rain image on Left.

where I_1, I_2 are the input sequences with spatial index $\mathbf{x}$. $\mathbf{u}$ is the flow vector with λ_s as a regularization parameter. We design our objective function by taking the residue map as an additional data constraint with corresponding weighting parameter:

$$\begin{aligned} E(I_1, I_2, \mathbf{u}) = (1-w) \| I_1(\mathbf{x}) - I_2(\mathbf{x}+\mathbf{u}) \|^2 \\ + w \| R_1(\mathbf{x}) - R_2(\mathbf{x}+\mathbf{u}) \|^2 \\ + \lambda_s(||\nabla \mathbf{u}||^2), \end{aligned} \quad (7)$$

where R_1, R_2 are the residue channel derived from the original rain image I_1, I_2 respectively. w is the weighting factor defined as follows:

$$w = \gamma \sqrt{(I_1^R - I_1^G)^2 + (I_1^G - I_1^B)^2 + (I_1^B - I_1^R)^2}, \quad (8)$$

where I_1^R, I_1^G, I_1^B are the RGB channels of image I_1 and γ is a scale parameter. Objects or scene with low level of color saturation will yield low intensity and low contrast in the residue channel. In the extreme case, white and gray objects in the scene would become black. Since low contrast

image will be susceptible to noise, we weigh the additional residue data constraint with w that is given by the Euclidean distance between the pixel color and mid-tone gray.

4.2. Piecewise-smooth + Fine-detail Decomposition

When rain is relatively heavy, detailed texture on the background is severely corrupted by the ubiquitous raindrops, and is difficult to recover by the regular ROF decomposition. In this heavily degraded scenario, we resort to a more impoverished and coarse version of the scene to supply the constraint on optical flow. This version of the scene will include the principal contours of the image. For this purpose, we decompose the rain image into a piecewise-smooth layer describing the principal regions of the image and a fine-detail layer containing the background texture, the raindrops, and the noise. Formally, the observed rain image I can be modeled as a linear combination of the piecewise-smooth layer J and the fine-detail layer L:

$$I = J + L \tag{9}$$

Our method extracts the piecewise-smooth part by restricting the amount of gradient magnitude:

$$C(J) = \#\{i \mid |\partial x J_i| + |\partial y J_i| \neq 0\} \tag{10}$$

where J is the piecewise-smooth background component and i is the pixel index of the image. $|\partial x J_i|$ is defined as the sum of gradient magnitudes in RGB channels. Therefore, this constraint is effectively the $L0$-norm of the gradients in J. Meanwhile, the piecewise-smooth background layer should be close to the observed image; thus the decomposition constraint can be expressed in the following energy minimization form:

$$\min_J \parallel I - J \parallel^2 + \parallel \nabla J \parallel_0 \tag{11}$$

$$s.t. \quad \forall i \quad 0 \leq J_i \leq I_i.$$

where $\nabla = (\partial x, \partial y)^T$. Hence, taking the optical flow into consideration, we obtain the following energy minimization problem as our formulation:

$$\begin{aligned} E(I_1, I_2, J_1, J_2, \mathbf{u}) &= (\|J_1(\mathbf{x}) - J_2(\mathbf{x}+\mathbf{u})\|^2) \\ &+ \lambda_s(||\nabla \mathbf{u}||^2) + \alpha(||I_1 - J_1||^2 + ||I_2 - J_2||^2) \\ &+ \beta(||\nabla J_1||_0 + ||\nabla J_2||_0) \end{aligned} \tag{12}$$

where I_1 I_2 are two input rain frames. J_1, J_2 are the piecewise-smooth background layers of the two frames respectively. λ_s is the smoothness parameter for the flow $\mathbf{u}$. β is the parameter controlling the gradient threshold. The higher the β , the fewer boundaries in the piecewise-smooth background layer.

5. Optimization

5.1. Overall Objective Function

By introducing the residue channel R_1, R_2 and its corresponding weight parameter w, our overall objective function is:

$$\begin{aligned} E(I_1, I_2, J_1, J_2, \mathbf{u}) &= \lambda_d[(1-w) \parallel J_1(\mathbf{x}) - J_2(\mathbf{x}+\mathbf{u}) \parallel^2 \\ &+ w \parallel R_1(\mathbf{x}) - R_2(\mathbf{x}+\mathbf{u}) \parallel^2] + \lambda_s(||\nabla \mathbf{u}||^2) \\ &+ \alpha(||I_1 - J_1||^2 + ||I_2 - J_2||^2) \\ &+ \beta(||\nabla J_1||_0 + ||\nabla J_2||_0) \end{aligned} \tag{13}$$

$$s.t. \quad 0 <= J_1 <= I_1 \quad 0 <= J_2 <= I_2$$

where R_1 and R_2 represent the residue channel maps of each frame correspondingly. Except for the gradients of the J layers, all the other terms are in $L2$-norm.

5.2. Alternating Minimization

In order to optimize our objective function, we iteratively solve the following sub-tasks given some initialization.

Sub-problem 1: Optical Flow Computation Given current piecewise-smooth background layers (J_1, J_2), we obtain the residue channel maps (R_1, R_2) and estimation the optical flow vector $\mathbf{u}$:

$$\begin{aligned} \min_{R_1, R_2, \mathbf{u}} \{&\lambda_d[(1-w) \parallel J_1(\mathbf{x}) - J_2(\mathbf{x}+\mathbf{u}) \parallel^2 \\ &+ w \parallel R_1(\mathbf{x}) - R_2(\mathbf{x}+\mathbf{u}) \parallel^2] + \lambda_s(||\nabla \mathbf{u}||^2)\} \end{aligned} \tag{14}$$

Sub-problem 2: Layer Separation Given the current optical flow $\mathbf{u}$, we compute the piecewise-smooth background layer $J_1, and J_2$ separately:

$$\begin{aligned} \min_{J_1}\{&\lambda_d \parallel J_1(\mathbf{x}) - J_2(\mathbf{x}+\mathbf{u}) \parallel^2 + \alpha(||I_1 - J_1||^2 \\ &+ \beta(||\nabla J_1||_0\} \end{aligned} \tag{15}$$

$$\begin{aligned} \min_{J_2}\{&\lambda_d \parallel J_1(\mathbf{x}) - J_2(\mathbf{x}+\mathbf{u}) \parallel^2 + \alpha(||I_2 - J_2||^2 \\ &+ \beta(||\nabla J_2||_0\} \end{aligned} \tag{16}$$

We first estimate the optical flow by assuming the original rain input image as the piecewise-smooth background layer. The estimation gives us an initial flow field. Then we solve the layer separation problem with the flow field. Eq.(15),(16) are non-convex because of the $L0$-norm terms. Therefore, we adopt the alternating optimization strategy from [19], by introducing two auxiliary variables to decouple the background gradient term and the quadratic terms. Although there is no guarantee for convergence to this non-convex problem, with initialization as proposed above, this algorithm performs well in practice. In our experiments, we have run our algorithm on hundreds of different rain scenes and it showed a good convergence.

Algorithm 1 Piecewise-smooth Detail Decomposition

Input: Image sequence I_1, I_2, regularization parameter λ_s, parameter α, β, maximum iteration M.
Initialization: Assign $J_1^{(0)} \leftarrow I_1, J_2^{(0)} \leftarrow I_2$. Estimate initial flow $\mathbf{u}^0 \leftarrow J_1^{(0)}, J_2^{(0)}$
for iteration i = 1, ..., M **do**
    Warp $J_1^{(i)} \rightarrow J_1'^{(i)}, J_2^{(i)} \rightarrow J_2'^{(i)}$ using $\mathbf{u}^0$
    Compute $J_1^{(i+1)} \leftarrow J_2'^{(i)}, I_1$
    Compute $J_2^{(i+1)} \leftarrow J_1'^{(i)}, I_2$
    Estimate Flow $\mathbf{u}^{(i+1)} \leftarrow J_1^{(i+1)}, J_2^{(i+1)}$
end for
Output: Estimated flow field $\mathbf{u}^{(M)}$

6. Experiments

We evaluate our method by comparing it with representative existing methods [16] [5] [12] on both synthetic data and real rain data. For synthetic data, we rendered rain streaks following the rain model from [8] on the widely used Middlebury optical flow dataset. The rain streaks are generated separately and overlaid on top of the Middlebury sequences according to Eq.(1). The rain streaks' strength and orientation are randomly rendered for each image in the sequence. The rain streaks' strength τ variates from 0 to 0.5. We use angle ω to represent the degree the rain streaks deviates from the vertical direction. In this experiments, ω is in the range of [-5°, 5°]. For real rain data, For the real rain data, we captured more than 1000 real rain images with different rain levels, containing both rain accumulation and rain streaks. The camera we used to capture rain images is NIKON D90 with focal length 45mm. All the experiments are run on a desktop with Intel(R) 12-core 3.06GHz CPU. The time taken to process an image pair with 388x584 image resolution is around 1 minute.

6.1. Synthetic Data Results

In this experiment, we first evaluate our algorithm on the synthetic Middlebury data rendered with rain streaks. The evaluation metric is the average end-point-error (AEPE), which is widely used in the optical flow community. We also compare our algorithm with some state-of-the-art methods, i.e. Classic+NL [16], LDOF [5], and SP-MBP [12]. For a more fair comparison, we utilize the single-image deraining algorithm [13] as a pre-processing for these algorithms. We also compare our algorithm with these algorithms with de-rain pre-processing. The quantitative results are shown in Table 1. We also select 'Dimetrodon' sequence from the Middlebury dataset and present qualitative results in Fig. 6.

In Fig. 6, Classic+NL fails to produce the correct flow field because the Classic+NL relies on brightness constancy constraint which is violated under the appearance of the rendered rain streaks. We observe the classic + NL result is separated into multiple regions in which the flow are trapped locally. The reason is that the rendered rain streaks produce extra boundaries that prevents the flow in each region to propagate across. With de-rain method as a pre-processing, Classic+NL produces a smoother result with larger blocks of local flow fields. Even though de-rain algorithm significantly removes the rain streaks from the input images, it generates artifacts in its output image, such as color change and background high frequency details loss. In this case, the brightness constancy constraint is also violated. SPM-BP also performs poor with the presence of rain streaks. The result of SPM-BP method also contains multiple regions of local flow field with same direction. The erroneous flow field shows that patch-match based method produces similar results as Classic+NL. The reason is that patch-match based method is also based on brightness constancy assumption. With the appearance of rain streak, each patch cannot find appropriate candidates due to the disruption of the rain streaks. With de-rain pre-processing added, patch-match also cannot correctly recover the flow field. However, LDOF performs better on the rain sequences because of the feature match. Though with rain streaks rendered, the background feature are still quite clear and hence reliable to provide confident matching. In contrast, our method produces the closest result to the ground-truth. Quantitatively, Table 1 shows that our method outperforms all the other algorithms and its accuracy is even competitive to other algorithms performing on the original Middlebury dataset.

Sequence	Classic+NL [16]	LDOF [5]	SPM-BP [12]	Ours
Rain	1.20	0.95	1.16	**0.30**
De-Rain	0.90	0.90	0.93	-

Table 1: Average end-point-error on rain rendered Middlebury dataset. 'de-rain sequence' refers to the images after applying Yu et al.'s [13] rain streak removal method.

6.2. Real Data Results

We also compare our algorithm with the aforementioned methods on real rain images. Some results are shown in Fig. 7. In order to better visualize the object movements, we show the overlaid images rather than the original images in the first column of Fig. 7. The original image sequence can be found in the supplementary material. In Fig. 7, rows (a)-(f) are examples that contain noticeable rain accumulation as well as rain streaks. Rows (g),(h) show examples with rain streaks only. From these results, we can evaluate the performance of each method on scenes with rain streaks and rain accumulation. In general, these methods can estimate

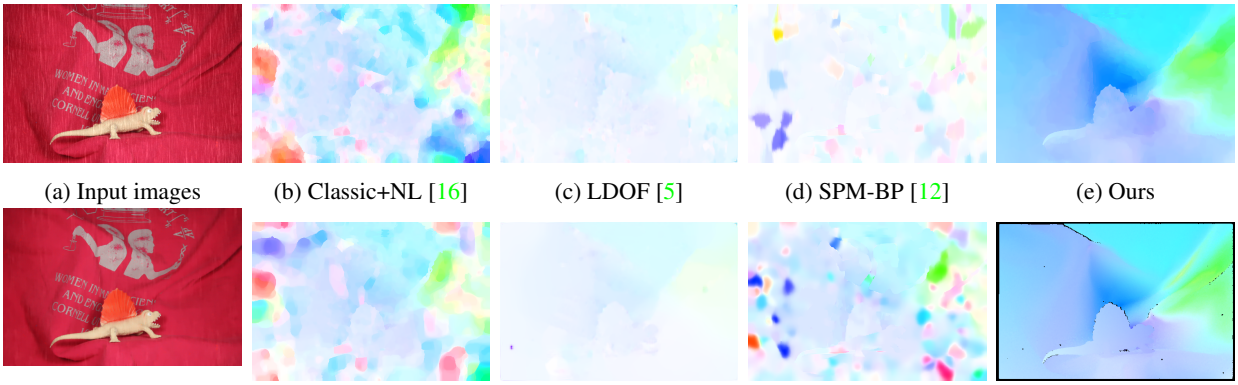

(a) Input images (b) Classic+NL [16] (c) LDOF [5] (d) SPM-BP [12] (e) Ours

(f) Input images after de-rain [13] pre-processing (g) Classic+NL [16] (h) LDOF [5] (i) SPM-BP [12] (j) Ground-Truth

Figure 6: Qualitative results of algorithms on rain rendered Middlebury sequence 'Dimetrodon'. (**Best viewed on screen**)

optical flow under slight rain robustly (*i.e.*, the rain streaks are very sparse and there is almost no rain accumulation). However, when the rain is heavier, the rain streaks become more apparent and these methods start to fail.

Classic+NL method is observed to be sensitive to the rain streaks and fails to produce smooth background in all the test examples since the brightness constancy constraint it uses is violated in rainy scenes. The LDOF method also cannot handle the rain accumulation effect with strong rain streak. In Fig. 7 (c) and (d), the scene background is totally static and only the bus, the pedestrians, and the top left tree branches are moving. However, LDOF method generates sporadic flows across the entire flow field. The reason is that it erroneously selects the rain streaks as feature matching points, thus results in incorrect flow fields. Patch-match based method like SPM-BP can also be affected by the rain streaks and accumulation. In Fig. 7 (h), the image background is totally static and rain streaks movement can be observed on top left of the image. SPM-BP method is affected by the movements of the rain streaks and produces massive inaccurate flow in those regions. It also fails to generate globally smooth flow when the scene contains significant rain accumulation (see Fig. 7 (c)). In contrast, our method is able to differentiate the rain streaks' movements and the background objects' movements. In the case of heavy rain accumulation (Fig. 7 (c) and (d)), our method successfully captures the movements of the bus and the pedestrians, and produces a globally smooth background flow field. In Fig. 7 (g), our method successfully recovers the motion of the person under rain streaks and generates a smooth background motion without losing the sharp motion boundaries of that person.

7. Conclusion

We have introduced an algorithm for optical flow estimation in rainy scenes. To come to grips with the rain streaks and rain accumulation effect, we propose the residue channel and a layer separation scheme respectively. In our experiments, the quantitative and qualitative results demonstrate that our method outperforms all the other state-of-the-art methods on both synthetic and real rain data sets. In our future work, we will apply our method to other dynamic weather phenomena such as snow and sleet.

References

[1] *Robust Optical Flow Estimation of Double-Layer Images under Transparency or Reflection*. IEEE Computer Society, 2016. 2

[2] J. L. Barron, D. J. Fleet, and S. S. Beauchemin. Performance of optical flow techniques. *Int. J. Comput. Vision*, 12(1):43–77, Feb. 1994. 2

[3] M. J. Black and P. Anandan. The robust estimation of multiple motions. *Comput. Vis. Image Underst.*, 63(1):75–104, Jan. 1996. 2

[4] T. Brox, A. Bruhn, N. Papenberg, and J. Weickert. High accuracy optical flow estimation based on a theory for warping. In *European Conference on Computer Vision (ECCV)*, volume 3024 of *Lecture Notes in Computer Science*, pages 25–36. Springer, May 2004. 2

[5] T. Brox and J. Malik. Large displacement optical flow: descriptor matching in variational motion estimation. *IEEE Transactions on Pattern Analysis and Machine Intelligence*, 33(3):500–513, 2011. 6, 7, 8

[6] C. B. Choy, J. Gwak, S. Savarese, and M. Chandraker. Universal correspondence network. In *Advances in Neural Information Processing Systems 29*. 2016. 2

[7] A. Dosovitskiy, P. Fischer, E. Ilg, , V. Golkov, V. G. P. S. D. C. P. Husser, C. Hazirba, and T. Brox. Flownet: Learning optical flow with convolutional networks. In *IEEE International Conference on Computer Vision (ICCV)*, 2015. 2

[8] K. Garg and S. K. Nayar. Photorealistic rendering of rain streaks. *ACM Trans. Graph.*, 25(3):996–1002, July 2006. 6

[9] K. Garg and S. K. Nayar. Vision and rain. *Int. J. Comput. Vision*, 75(1):3–27, Oct. 2007. 3

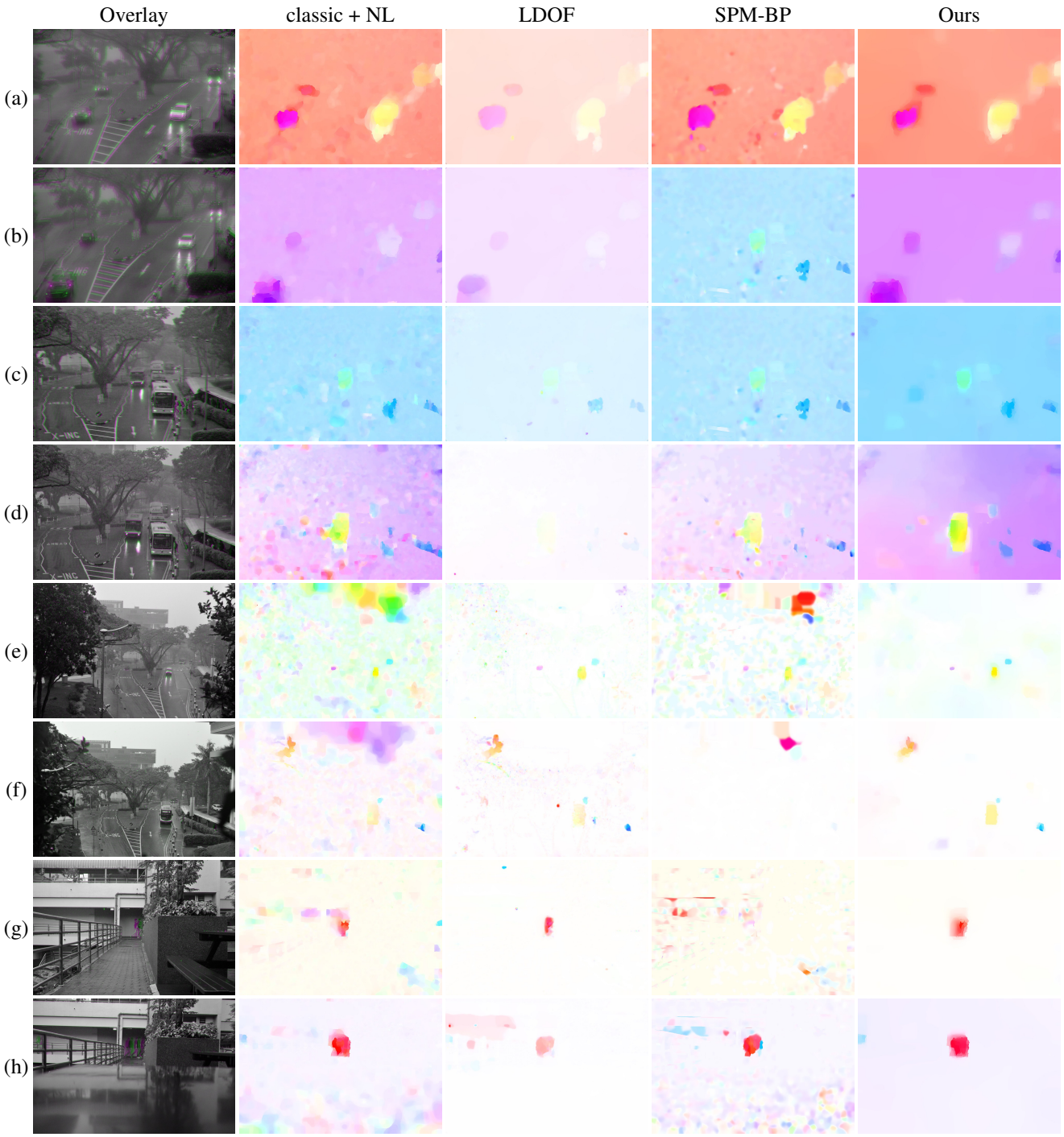

Figure 7: Method comparison on real rainy scenes with different severity level. In each row left to right: overlaid image pair, flow field of classic+NL [16], flow field of LDOF [5], flow field of SPM-BP [12] and flow field of the proposed method of this paper. In order to show object movement in the image, we put overlaid image pair rather than the original image (**Best viewed on screen**).

[10] E. Ilg, N. Mayer, T. Saikia, M. Keuper, A. Dosovitskiy, and T. Brox. Flownet 2.0: Evolution of optical flow estimation with deep networks. *CoRR*, abs/1612.01925, 2016. 2

[11] L. W. Kang, C. W. Lin, and Y. H. Fu. Automatic single-image-based rain streaks removal via image decomposition. *IEEE Transactions on Image Processing*, 21(4):1742–1755,

April 2012. 2, 3

[12] Y. Li, D. Min, M. S. Brown, M. N. Do, and J. Lu. Spm-bp: Sped-up patchmatch belief propagation for continuous mrfs. In *2015 IEEE International Conference on Computer Vision (ICCV)*, pages 4006–4014, Dec 2015. 1, 6, 7, 8

[13] Y. Li, R. T. Tan, X. Guo, J. Lu, and M. S. Brown. Rain streak removal using layer priors. In *The IEEE Conference on Computer Vision and Pattern Recognition (CVPR)*, June 2016. 2, 3, 6, 7

[14] Y. Mileva, A. Bruhn, and J. Weickert. *Illumination-Robust Variational Optical Flow with Photometric Invariants*, pages 152–162. Springer Berlin Heidelberg, Berlin, Heidelberg, 2007. 2

[15] L. I. Rudin, S. Osher, and E. Fatemi. Nonlinear total variation based noise removal algorithms. In *Proceedings of the Eleventh Annual International Conference of the Center for Nonlinear Studies on Experimental Mathematics : Computational Issues in Nonlinear Science: Computational Issues in Nonlinear Science*, pages 259–268, Amsterdam, The Netherlands, The Netherlands, 1992. Elsevier North-Holland, Inc. 2

[16] D. Sun, S. Roth, and M. J. Black. Secrets of optical flow estimation and their principles. In *IEEE Conf. on Computer Vision and Pattern Recognition (CVPR)*, pages 2432–2439. IEEE, June 2010. 1, 2, 6, 7, 8

[17] W. Trobin, T. Pock, D. Cremers, and H. Bischof. An unbiased second-order prior for high-accuracy motion estimation. In *Pattern Recognition, 30th DAGM Symposium, Munich, Germany, June 10-13, 2008, Proceedings*, pages 396–405, 2008. 2

[18] A. Wedel, T. Pock, C. Zach, H. Bischof, and D. Cremers. Statistical and geometrical approaches to visual motion analysis. chapter An Improved Algorithm for TV-L1 Optical Flow, pages 23–45. Springer-Verlag, Berlin, Heidelberg, 2009. 2

[19] L. Xu, C. Lu, Y. Xu, and J. Jia. Image smoothing via l0 gradient minimization. *ACM Transactions on Graphics (SIGGRAPH Asia)*, 2011. 5

[20] W. Yang, R. T. Tan, J. Feng, J. Liu, Z. Guo, and S. Yan. Joint rain detection and removal via iterative region dependent multi-task learning. *CoRR*, abs/1609.07769, 2016. 2, 3

[21] X. Zhang, H. Li, Y. Qi, W. K. Leow, and T. K. Ng. Rain removal in video by combining temporal and chromatic properties. In *2006 IEEE International Conference on Multimedia and Expo*, pages 461–464, July 2006. 3